



Published in final edited form as:

*Invest Radiol.* 2015 February ; 50(2): 101–107. doi:10.1097/RLI.000000000000106.

## High-Permittivity Thin Dielectric Padding Improves Fresh Blood Imaging of Femoral Arteries at 3T

Marc D Lindley<sup>1,2</sup>, Daniel Kim<sup>2</sup>, Glen Morrell<sup>2</sup>, Marta E Heilbrun<sup>2</sup>, Pippa Storey<sup>3</sup>, Christopher J Hanrahan<sup>2</sup>, and Vivian S Lee<sup>2</sup>

<sup>1</sup>Department of Physics, University of Utah, 201 Presidents Cir, Salt Lake City, Utah, USA

<sup>2</sup>UCAIR, Department of Radiology, University of Utah, 201 Presidents Cir, Salt Lake City, Utah, USA

<sup>3</sup>Center for Biomedical Imaging, New York University School of Medicine, 660 First Avenue, New York, New York, USA

### Abstract

**Objectives**—Fresh blood imaging (FBI) is a useful non-contrast magnetic resonance angiography (NC-MRA) method for assessment of peripheral arterial disease (PAD), particularly in patients with poor renal function. Compared with 1.5T, 3T enables higher signal to noise ratio (SNR) and/or spatio-temporal resolution in FBI, as demonstrated successfully for the calf station. However, FBI of the thigh station at 3T has been reported to suffer from signal void in the common femoral artery of one thigh only due to the radial symmetry in transmit radio-frequency field ( $B_{1+}$ ) variation. We sought to increase the femoral arterial signal attenuated by  $B_{1+}$  variation in FBI at 3T using high permittivity dielectric padding.

**Materials and Methods**—We performed FBI of the thigh station in 13 human subjects at 3T to compare the following 3 settings: no padding, commercially available thick (~5 cm) dielectric padding, and high-permittivity thin (~2 cm) dielectric padding.  $B_{1+}$  mapping was also performed in the common femoral arteries to characterize the radial symmetry in  $B_{1+}$  variation and quantify the improvement in  $B_{1+}$  excitation. We characterized the impact of radial symmetry in  $B_{1+}$  variation on the FBI signal and FBI MRA of the right common femoral artery using quantitative (i.e., contrast-to-noise ratio (CNR)) and qualitative (i.e., conspicuity) analyses.

**Results**—The radial symmetry in  $B_{1+}$  variation attenuates signal in the right common femoral artery, which can be partially improved with commercial padding and improved further with high permittivity padding. Averaging the results over 13 subjects, the  $B_{1+}$ , CNR and conspicuity scores in the right common femoral artery were significantly better with high-permittivity padding than with commercial padding and baseline ( $p < 0.001$ ).

**Conclusions**—Our study shows that high-permittivity dielectric padding can be used to increase the femoral arterial signal attenuated by  $B_{1+}$  variation in FBI at 3T.

Corresponding author: Marc Lindley, UCAIR, University of Utah, 729 Arapleen Dr, Salt Lake City, UT 84108, marcldindley@gmail.com.

This work was presented in part at the 2014 SCMR conference

## Keywords

Peripheral arterial disease; non-contrast MRA; dielectric padding;  $B_1+$  inhomogeneity; fresh blood imaging

---

## Introduction

Peripheral arterial disease (PAD) is a chronic disease that affects over 5 million Americans and is projected to affect over 7 million adults in the US by year 2020 [1]. Imaging plays an important role in diagnosis and guiding therapy. Contrast-enhanced magnetic resonance angiography (MRA) is clinically indicated as a test for noninvasive diagnosis and evaluation of PAD [2, 3]. However, gadolinium-based contrast agents have been associated with nephrogenic systemic fibrosis in patients with renal insufficiency [4, 5], which is a major concern given that approximately 40% of patients with PAD have renal insufficiency [6].

This safety concern has activated a renewed interest in non-contrast MRA (NC-MRA) methods [7-10]. One such method is fresh blood imaging (FBI) which is based on subtraction of two 3D fast spin-echo (FSE) acquisitions at two different cardiac phases [9, 10]. The first FSE scan is acquired during diastole, in which both the arteries and veins appear bright. The second scan is acquired during systole, in which the veins appear bright and the arteries appear dark due to flow-induced signal dephasing. By subtracting these two images, by which veins and background cancel out, bright-blood angiograms can be obtained. FBI of peripheral vasculature has been shown to work effectively for both the thigh and calf stations at 1.5T [11-14].

Widening the availability of FBI to all clinical scanners, including 3T, is important since approximately 1/3 of clinical MR scanners in the US are 3T, and since 3T enables higher signal to noise ratio (SNR) and/or spatio-temporal resolution, as demonstrated successfully for the calf station at 3T [8, 15]. Our preliminary analysis in a few human subjects indicates that 3T, as compared with 1.5T, improves SNR in the thigh station by approximately 50%. However, FBI of the thigh station at 3T has been reported to suffer from signal void in the common femoral artery of one thigh only due to the radial symmetry in transmit radio-frequency (RF) field ( $B_1+$ ) variation [16]. Given that this problem is not well understood in the MRA field, in this study, we characterize the radial symmetry in  $B_1+$  variation and its impact on the FSE signal and FBI MRA.

Several methods are commercially available for compensating  $B_1+$  inhomogeneity, including  $B_1+$  shimming and parallel transmit RF technologies such as Philips *MultiTransmit*® (Philips, Eindhoven, The Netherlands) and Siemens *TrueForm*® (Siemens Healthcare, Erlangen, Germany) which require expensive hardware. Similar to a typical runoff contrast-enhanced MRA protocol, our multi-station (abdomen, thigh, calf) NC-MRA protocol is based on 3D coronal image acquisitions with head-to-foot coverage on the order of 400-500 mm per station. This requirement necessitates a long-bore MRI system with large effective field of view (e.g., Tim Trio, Siemens), which is unfortunately not equipped with the *TrueForm*® technology. Therefore, we sought to compensate for  $B_1+$  variation in a long-bore 3T MRI system using high permittivity dielectric padding, which has been applied

for brain, body, and cardiac MRI applications [17-20]. Dielectric padding has a major advantage of being low in cost (~\$150) in comparison to B<sub>1+</sub> shimming and parallel transmit systems. The utility of high permittivity dielectric padding for FBI of the thigh station has not been evaluated until very recently in a preliminary analysis [21]. The objective of this study was to construct and evaluate high-permittivity dielectric padding for increasing the femoral arterial signal attenuated by B<sub>1+</sub> variation in FBI at 3T.

## Materials and Methods

### High Permittivity Dielectric Pad

High permittivity pad was constructed using barium titanate (Alfa Aesar, 99%, ~325 mesh) and distilled water and was heat-sealed in a polyethylene bag. An approximate ratio of 4:1 by weight (barium titanate to water) was used to achieve the appropriate saturated suspension [17, 20]. To evaluate the relative permittivity of the barium titanate mixture compared with commercially available pad, we performed the following simple experiment. Using two copper plates (~2 × 2 inches in dimensions), we measured the capacitance of a fixed distance with and without the padding. Using the equation describing the capacitance

$C = \epsilon_r \epsilon_0 \frac{A}{d}$ , where  $\epsilon_r$  is the relative permittivity,  $\epsilon_0$  is the electric constant ( $8.854 \times 10^{-12}$  F m<sup>-1</sup>),  $A$  is the area of the two plates, and  $d$  is the distance between the plates. This preliminary analysis showed that the barium titanate pad had approximately 9-fold higher permittivity than commercially available pad. We elected not to report the absolute value of each pad, because accurate measurement of permittivity requires a more complicated analysis that is beyond the scope of this study.

The barium titanate pad, now referred to as high-permittivity padding throughout this study, was constructed with in-plane dimensions of 38 × 20 cm to cover the right thigh and pelvis following the path of the femoral arteries and within the peripheral RF coil configuration. These pad dimensions and placement were determined empirically based on B<sub>1+</sub> mapping of the thigh and extensive experience with FBI of the thigh station at 3T. In a preliminary experiment, we compared the performances of three different pad thicknesses (1, 2, and 3 cm) in a volunteer to determine an optimal thickness, and the results (Figure 1) from this analysis showed that pad size of 38 × 20 × 2 cm produced optimal results (i.e., more even FBI signal between the left and right common femoral arteries). Thus, we used the pad size of 38 × 20 × 2 cm (weighing 3.7 kg) throughout this study.

### Human Subjects

Nine healthy volunteers (9 males, mean age = 33 ± 8 years) and four patients (3 males and 1 female, mean age = 65 ± 13 years) with PAD were studied with FBI. All subjects were positioned on the MR table in feet-first, supine orientation. This study was compliant with the Health Insurance Portability and Accountability Act and approved by the local Institutional Review Board. Written informed consent was obtained from all subjects.

## MRI Experiment

Imaging was performed on a whole-body 3T system (Tim Trio, Siemens Healthcare, Erlangen, Germany, maximum gradient strength = 40 mT/m; slew rate = 200 T/m/s). RF excitation was performed using the body coil. For signal reception, body matrix coil array (6 elements available), peripheral coil array (16 elements available), and spine coil array (24 elements available) were employed. For the thigh station alone, the number of elements used was 32 elements. For each subject, we performed FBI and rapid  $B_1+$  mapping [22] with three different settings: no padding, with commercial padding, and with high-permittivity padding. A commercially available dielectric pad (Siemens),  $37 \times 25 \times 5 \text{ cm}^3$ , with a weight of 2.9 kg, was compared, with the same placement as the custom made padding (Figure 2). For consistency, we used the same pad placement for all subjects, by using the peripheral matrix coil as the marker for positioning the bottom of the padding. Care was taken to ensure that transmit and receive RF settings were identical for the three experiments. The magnet isocenter was set consistently at the mid-thigh level for all subjects, as is typically done for our multi-station runoff MRA protocol.  $B_1+$  mapping was performed in an axial plane at the common femoral artery level in the same three settings as described above.

## Pulse Sequence

FBI of the thigh station was performed using the following relevant imaging parameters: scan time ~ 4 min, field of view 500 (readout encoding) mm  $\times$  425 (phase encoding) mm  $\times$  163-204 (partition encoding) mm, image acquisition matrix  $320 \times 276 \times 96$ -120, spatial resolution 1.3 mm  $\times$  1.3 mm  $\times$  1.7 mm, TR = one heart beat based on electrocardiogram, TE = 22 ms, constant refocusing flip angle =  $120^\circ$ , bandwidth = 781 Hz/pixel, echo train length = 136 and generalized autocalibrating partially parallel acquisitions (GRAPPA)[23] acceleration factor  $R = 1.7$  (accounting for 24 reference lines) in the left-right direction. For each subject, phase-contrast MRI was performed in an axial plane to determine the trigger delay for peak systolic flow in the femoral artery. Typical trigger delay typically ranged from 150 – 270 ms.

Contrast enhanced MRA was performed on each of 4 patients, as part of clinical MR examination, using the following relevant imaging parameters: scan time ~ 29 sec, field of view 500 mm  $\times$  406 mm  $\times$  134-168 mm, image acquisition matrix  $384 \times 234 \times 96$ -120, spatial resolution 1.3 mm  $\times$  1.7 mm  $\times$  1.4 mm, TR = 3.5, TE = 1.2 ms, flip angle =  $25^\circ$ , bandwidth = 781Hz/pixel, and actual GRAPPA acceleration factor  $R = 1.7$ . Gadoteridol (Bracco, Monroe Township, New Jersey) was administered via a power injector (MedRad, Warrendale, Pennsylvania), based on subject weight (~30 cc).

We used a previously described rapid  $B_1+$  mapping pulse sequence [22] based on ultra-fast gradient echo (TurboFLASH) readout with centric k-space ordering. Briefly, this sequence acquires a proton density image, PD, first and then waits adequate time for full magnetization recovery (e.g.,  $5 T_1 \sim 10 \text{ s}$ ). A second image, SS Pre, is then acquired using a magnetization preparation module followed immediately by the same TurboFLASH readout. The magnetization preparation module consists of a slice-selective RF pulse with nominal flip angle  $\alpha = 60^\circ$ ,  $\alpha^{\text{nom}}$ , and spoiler gradients. The relative  $B_1+$  value can be calculated using the following equation

$$\kappa = \cos^{-1} \frac{SS_{Pre}}{PD} / \alpha^{nom} \quad (1)$$

which provides a normalized  $B_{1+}$  map [22].

## Image Analysis

### Analysis 1: Radial Symmetry in $B_{1+}$ variation and its Impact on FSE Signal—

We quantified the radial symmetry in  $B_{1+}$  variation in the three acquisition settings (baseline, commercial padding, and high permittivity padding) and its impact on the FSE signal. We drew region-of-interest (ROI)s including the left and right common femoral arteries as shown in Figure 1. We reformatted the FSE images in the same plane as the  $B_{1+}$  map, and drew the corresponding ROI)s in the diastolic and systolic FSE images. To average the FSE signals over subjects, we first normalized the lower signal by the higher signal (control), and then averaged the normalized signal over subjects. This normalization is necessary since MRI signal is scaled differently for different subjects. The resulting normalized  $B_{1+}$  and FSE signals were compared between the padding settings.

### Analysis 2: Radial Symmetry in $B_{1+}$ variation and its Impact on MRA—

We quantified the impact of radial symmetry in  $B_{1+}$  variation on FBI MRA. Specifically, we quantified contrast-to-noise ratio (CNR) =  $(SI_{artery} - SI_{background\_Tissue}) / \text{noise}$ . Note that the signal intensity was determined from the subtracted images and noise was obtained from the diastolic images, since subtracted images have altered noise statistics. For each common femoral artery, we identified the bifurcation point and drew a rectangular contour with approximately 190 pixels ( $\sim 120 \text{ mm}^2$ ) to quantify the mean arterial signal. The same contour was then moved laterally to background tissue to quantify the mean background signal (see insert in Figure 3). For consistency, we used the same set of contours for the three scans. For noise estimation, we drew a circular contour with approximately 1900 pixels ( $\sim 1200 \text{ mm}^2$ ) in a signal-free region in diastolic images.

## Image Quality Assessment

Three radiologists with 11 years (XX), 6 years (YY), and 5 years (ZZ) of experience were asked to score in consensus the conspicuity of right and left common femoral arteries at the bifurcation level. The images were graded on a Likert scale of 1-5 (worst to best). The radiologists were blinded to image acquisition type and subject identity. To avoid bias, we made sure to crop out the padding in images.

## Statistical Analysis

For analysis 1, the mean  $B_{1+}$  and FSE signal were compared for the three groups using analysis of variance (ANOVA), and with Bonferroni correction to compare each pair of groups. Similarly, for analysis 2, the mean CNR values for the three groups were compared using ANOVA, and with Bonferroni correction to compare each pair of groups. For image quality analysis, the mean apparent image quality scores for the three groups were compared using Kruskal-Wallis test, and with Bonferroni correction to compare each pair of groups. A

p value < 0.05 was considered statistically significant. All statistical analyses were performed using Matlab (R2009a, Statistics Toolbox, The MathWorks, Inc., Natick, MA).

## Results

### Analysis 1: Radial Symmetry in $B_{1+}$ variation and its Impact on FSE Signal

Figure 2 shows representative  $B_{1+}$  maps displaying the radial symmetry in  $B_{1+}$  variation. Note that anterior-right ROI shows lower  $B_{1+}$  compared with anterior-left ROI without any padding. These  $B_{1+}$  variation patterns translate to the corresponding signal variations in diastolic FSE images as shown in Figure 2 (systolic FSE images not shown due to space constraint, but similar trends were observed and summarized in Table 1). The attenuated  $B_{1+}$  and FSE signal in the first ROI (anterior-right) are partially improved with commercial padding and improved further with high permittivity padding, as shown. Averaging the results over 13 subjects, the mean  $B_{1+}$  for the anterior-right ROI is significantly different ( $p < 0.0001$ ) between the three padding settings, where the  $B_{1+}$  values for high permittivity padding were significantly higher than those for commercial padding and baseline. Normalized  $B_{1+}$  for the anterior-left ROI was not different between the groups ( $p > 0.2$ ). The corresponding FSE signals showed similar trends in statistics (Table 2), where the anterior-right ROI was significantly different between the three groups and within each pair of groups ( $p < 0.0001$ ), and the anterior-left ROI was not different between the baseline and commercial padding ( $p > 0.2$ ), but was different between the high permittivity padding and the other two groups ( $p < 0.001$ ).

### Analysis 2: Radial Symmetry in $B_{1+}$ Variation and its Impact on MRA

Figure 3 shows representative maximum-intensity-projection (MIPs) of two different volunteers using FBI with different dielectric padding settings. In both subjects, compared with baseline, the signal in the right common femoral artery was increased partially using commercial dielectric padding and increased further using high-permittivity padding. The left femoral artery values remained consistent throughout the tests. Figure 4 shows representative MIPs of a PAD patient. This patient's MRA results were consistent with the volunteer results shown in Figure 3 (i.e., progressive improvement with commercial and then high permittivity padding).

Averaging the results over 13 subjects (Table 3), CNR of the right common femoral artery on FBI MRA was significantly ( $p < 0.001$ ) improved with the high permittivity padding ( $82 \pm 15$ ), compared to no padding ( $12 \pm 2$ ) and commercial padding ( $33 \pm 8$ ). Similarly, the conspicuity score of the right common femoral artery was significantly ( $p < 0.001$ ) improved with the high permittivity padding ( $4.3 \pm 0.8$ ), compared to no padding ( $1 \pm 0$ ) and commercial padding ( $2.5 \pm 1.0$ ). We note non-significant differences in the CNR and conspicuity scores for the left common artery (see Table 3).

## Discussion

This study characterizes the radial symmetry in  $B_{1+}$  variation that causes attenuation of femoral arterial signal in FBI of one thigh (right side if patient is positioned on the MR table with feet-first, supine orientation). This study also demonstrates that high-permittivity thin

dielectric padding can be used to increase the signal of the right common femoral artery in FBI at 3T. The  $B_{1+}$ , CNR, and image quality scores showed greater improvements with the high permittivity dielectric padding than commercial dielectric padding.

High permittivity dielectric padding provides a robust and inexpensive solution to increase the femoral arterial signal attenuated by the radial symmetry in  $B_{1+}$  variation at 3T. Unlike more expensive hardware solutions such as parallel RF transmit and  $B_{1+}$  shimming, dielectric padding can be fabricated easily by the user, typically at a cost around \$150 for the dimensions described in this study. Commercial padding used in this study increased the signal partially, but the amount of signal enhancement was insufficient to produce adequate FBI images of the right common femoral artery. Additionally, the thickness of commercial padding (5 cm) is less comfortable for patients and can limit proper positioning of the coil(s), especially in patients with high body mass index. High permittivity dielectric padding used in this study was only 2 cm thick, and has the clear advantage of providing more patient comfort and minimizing the gap between the coil and patient body.

The padding used in this study is a passive  $B_{1+}$  correction method. As such, the resulting performance is influenced by padding size and placement. We determined the size and placement empirically to yield good results over a wide range of body weights. For other applications, one may need to adapt the size and placement for optimal results. To account for different body sizes, one could make several padding sets with different sizes to achieve tailored results. We note that the particular padding size used in this study improved the quality of FBI of the thigh station over a wide range of body weight (63 to 95 kg). Nonetheless, additional studies in patients with different body mass indices with PAD is warranted to further validate the utility of high permittivity dielectric padding for increasing the signal in FBI of the thigh region at 3T. We note that the radial symmetry in  $B_{1+}$  variation affects only one thigh. In this study, with subjects positioned on the MR table with feet-first, supine orientation, the  $B_{1+}$  variation pattern attenuated signal in the right common femoral artery. We note that if the subject is positioned with head-first, supine orientation then the  $B_{1+}$  variation pattern will attenuate signal in the left common femoral artery. Thus, a user needs to consider the subject orientation on the MR table and apply the dielectric padding on the correct side. We note that CNR values reported in this study are not true values, since it is not feasible to determine the true image noise from GRAPPA images [23]. Since the three acquisitions used the same imaging parameters, except for the padding, we elected to calculate noise as the standard deviation in a signal free region, and use that same noise estimate to calculate the CNR for all three acquisitions for each subject. While the calculated CNR may not truly reflect absolute CNR, it is adequate for comparing the three acquisitions: no padding, commercial padding, and high-permittivity padding.

## Conclusion

This study shows that the radial symmetry in  $B_{1+}$  variation attenuates the femoral arterial signal of FBI in one thigh only. This study also shows that high permittivity thin dielectric padding can be used to increase the attenuated signal of the right common femoral artery in FBI at 3T.

## Acknowledgments

Grant support: National Institutes of Health (HL092439; HL116895-01A1)

This work is related to the US patent 8,334,691 (Ultra fast magnetic resonance imaging method and apparatus for non-contrast agent MR angiography using electrocardiograph or pulse triggered half fourier turbo spin echo-based acquisition with variable flip angle evolution and high resolution).

## References

1. Selvin E, Erlinger TP. Prevalence of and risk factors for peripheral arterial disease in the United States: results from the National Health and Nutrition Examination Survey, 1999-2000. *Circulation*. 2004; 110:738–43. [PubMed: 15262830]
2. Ho KY, Leiner T, de Haan MW, et al. Peripheral vascular tree stenoses: evaluation with moving-bed infusion-tracking MR angiography. *Radiology*. 1998; 206:683–92. [PubMed: 9494486]
3. Al-Qaisi M, Nott DM, King DH, et al. Imaging of peripheral vascular disease. *Reports in Medical Imaging*. 2009; 2:25–34.
4. Runge VM. Gadolinium and nephrogenic systemic fibrosis. *American Journal of Roentgenology*. 2009; 192:W195–W6. [PubMed: 19304681]
5. Collidge TA, Thomson PC, Mark PB, et al. Gadolinium-enhanced MR Imaging and Nephrogenic Systemic Fibrosis: Retrospective Study of a Renal Replacement Therapy Cohort1. *Radiology*. 2007; 245:168–75. [PubMed: 17704357]
6. Tranche-Iparraguirre S, Marin-Iranzo R, Fernandez-de Sanmamed R, et al. Peripheral arterial disease and kidney failure: a frequent association. *Nefrologia*. 2012; 32:313–20. [PubMed: 22508143]
7. Hodnett PA, Koktzoglou I, Davarpanah AH, et al. Evaluation of peripheral arterial disease with nonenhanced quiescent-interval single-shot MR angiography. *Radiology*. 2011; 260:282–93. [PubMed: 21502384]
8. Li D, Lin J, Yan F, et al. Unenhanced calf MR angiography at 3.0 T using electrocardiography-gated partial-fourier fast spin echo imaging with variable flip angle. *Eur Radiol*. 2011; 21:1311–22. [PubMed: 21153825]
9. Wedeen VJ, Meuli RA, Edelman RR, et al. Projective imaging of pulsatile flow with magnetic resonance. *Science*. 1985; 230:946–8. [PubMed: 4059917]
10. Miyazaki M, Sugiura S, Tateishi F, et al. Non-contrast-enhanced MR angiography using 3D ECG-synchronized half-Fourier fast spin echo. *J Magn Reson Imaging*. 2000; 12:776–83. [PubMed: 11050650]
11. Lim RP, Fan Z, Chatterji M, et al. Comparison of nonenhanced MR angiographic subtraction techniques for infragenual arteries at 1.5 T: a preliminary study. *Radiology*. 2013; 267:293–304. [PubMed: 23297320]
12. Hoey ET, Ganeshan A, Puni R, et al. Fresh blood imaging of the peripheral vasculature: an emerging unenhanced MR technique. *AJR American journal of roentgenology*. 2010; 195:1444–8. [PubMed: 21098208]
13. Nakamura K, Miyazaki M, Kuroki K, et al. Noncontrast-enhanced peripheral MRA: technical optimization of flow-spoiled fresh blood imaging for screening peripheral arterial diseases. *Magn Reson Med*. 2011; 65:595–602. [PubMed: 20872867]
14. Storey P, Lim RP, Kim S, et al. Arterial flow characteristics in the presence of vascular disease and implications for fast spin echo-based noncontrast MR angiography. *J Magn Reson Imaging*. 2011; 34:1472–9. [PubMed: 21959828]
15. Haneder S, Attenberger UI, Riffel P, et al. Magnetic resonance angiography (MRA) of the calf station at 3.0 T: intraindividual comparison of non-enhanced ECG-gated flow-dependent MRA, continuous table movement MRA and time-resolved MRA. *Eur Radiol*. 2011; 21:1452–61. [PubMed: 21274715]
16. Storey, P.; Lee, V.; Sodickson, D., et al. B1 inhomogeneity in the thigh at 3T and implications for peripheral vascular imaging; Proceedings of the 17th Annual Meeting of ISMRM; Honolulu, Hawaii, USA. 2009; p. 425



17. Teeuwisse WM, Brink WM, Haines KN, et al. Simulations of high permittivity materials for 7 T neuroimaging and evaluation of a new barium titanate-based dielectric. *Magn Reson Med.* 2012; 67:912–8. [PubMed: 22287360]
18. Haines K, Smith NB, Webb AG. New high dielectric constant materials for tailoring the B1+ distribution at high magnetic fields. *Journal of magnetic resonance.* 2010; 203:323–7. [PubMed: 20122862]
19. Brink WM, Webb AG. High permittivity pads reduce specific absorption rate, improve B homogeneity, and increase contrast-to-noise ratio for functional cardiac MRI at 3 T. *Magn Reson Med.* 2014; 71:1632–40. [PubMed: 23661547]
20. de Heer P, Brink WM, Kooij BJ, et al. Increasing signal homogeneity and image quality in abdominal imaging at 3 T with very high permittivity materials. *Magn Reson Med.* 2012; 68:1317–24. [PubMed: 22851426]
21. Lindley MD, Kim D, Morrell G, et al. High-permittivity thin dielectric pad improves peripheral non-contrast MRA at 3T. *Journal of Cardiovascular Magnetic Resonance.* 2014; 16:P166.
22. Chung S, Kim D, Breton E, et al. Rapid B1+ mapping using a preconditioning RF pulse with TurboFLASH readout. *Magn Reson Med.* 2010; 64:439–46. [PubMed: 20665788]
23. Griswold MA, Jakob PM, Heidemann RM, et al. Generalized autocalibrating partially parallel acquisitions (GRAPPA). *Magn Reson Med.* 2002; 47:1202–10. [PubMed: 12111967]

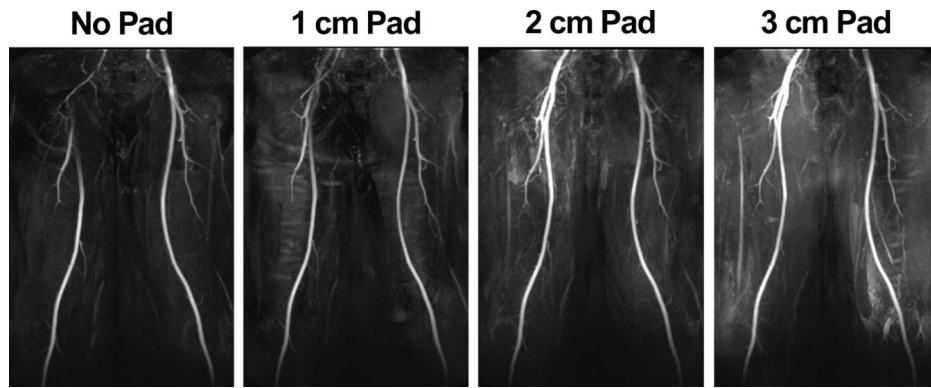


**Figure 1.**

MIPs of a volunteer with three different high-permittivity pad thicknesses: 1 cm (second column), 2 cm (third column), and 3 cm (fourth column). For reference, a MIP without padding is also shown (first column). All four MIPs were displayed in identical grayscale. Pad placement was on the upper-thigh to the pelvis following the path of the femoral arteries. Based on this preliminary analysis, we used the 2 cm thick pad throughout this study.

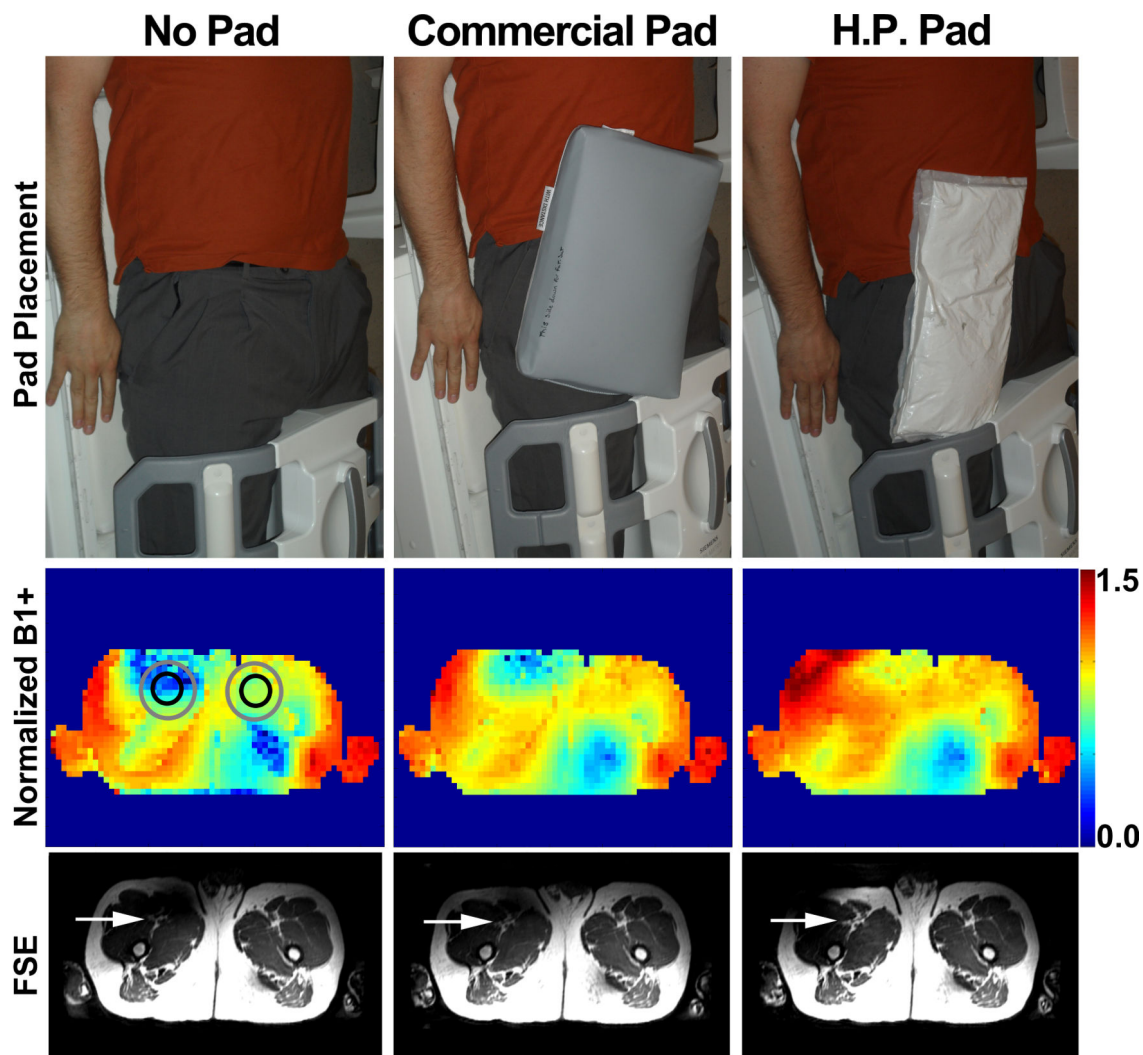


**Figure 2.**

FBI of the thigh station settings (row 1): no padding (left), commercially available padding (middle), and high permittivity padding (right). The pad placement was on the upper-thigh to the pelvis following the path of the femoral arteries. This placement was consistent from subject to subject with the peripheral coil configuration as shown. The subject's head is toward the top of the image. Corresponding normalized  $B_1+$  maps (row 2) and reformatted FSE images (row 3): baseline (left), commercial padding (middle), and high permittivity padding (right). At baseline, the radial symmetry in  $B_1+$  variation reduces  $B_1+$  in the anterior-right ROI (gray circle) corresponding to the right common femoral artery (black circle).  $B_1+$  in the anterior-right ROI is partially improved with commercial padding and improved further with high permittivity padding. Similar trends are shown in the FSE images (displayed in identical grayscales). Red arrows point to the right common femoral artery.

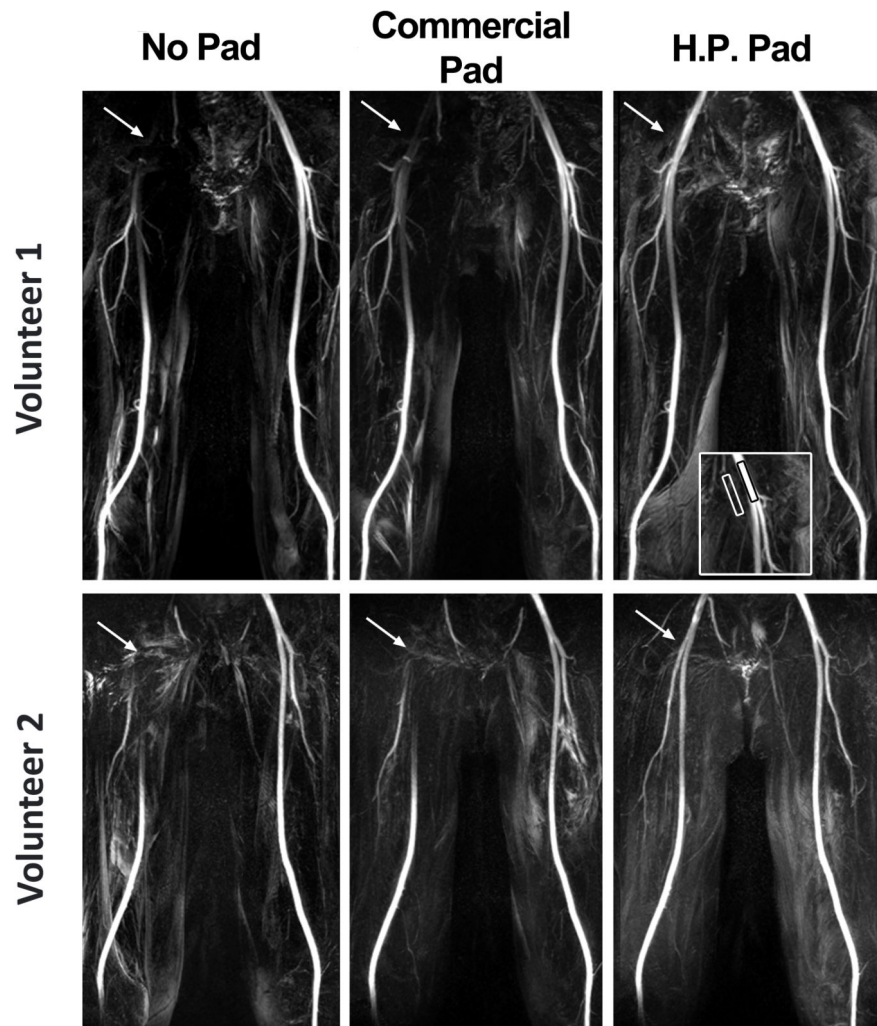


**Figure 3.** Representative MIPs of from two volunteers, volunteer 1 on top and volunteer 2 on bottom, with three different settings: baseline (left), commercial dielectric padding (middle), and high-permittivity dielectric padding (right). Compared with baseline and commercial dielectric padding, high-permittivity dielectric padding significantly increased signal around the bifurcation point of the common femoral artery. MIPs displayed in identical grayscales per subject.

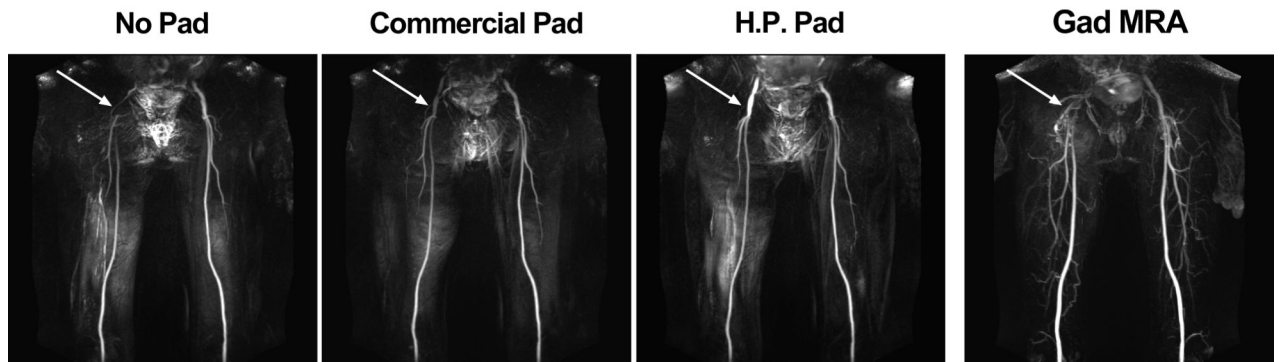


**Figure 4.**

Representative MIPs of a patient with infrarenal abdominal aortic aneurysm and subsequent an endovascular graft device: FBI without padding (first column), FBI with commercially padding (second column), FBI with high permittivity padding (third column), and contrast-enhanced MRA (fourth column). Patient has an endovascular graft, which caused image artifact at the top of the image, near the bladder. FBI MIPs are displayed with identical grayscale.

**Table 1**

Mean normalized  $B_{1+}$  in an axial plane of the thigh station. Reported values represent mean  $\pm$  standard deviation.  $B_{1+}$  in the anterior-right ROI was significantly different between the three groups and within each pair of groups ( $p < 0.0001$ ).  $B_{1+}$  in the anterior-left ROI was different between the high permittivity padding and the other two groups ( $p < 0.001$ ), but the baseline and commercial padding were not different ( $p > 0.2$ ).

Pad Setting		Baseline	Commercial Pad	High Permittivity Pad
Normalized $B_{1+}$	Right	$0.62 \pm 0.17$	$0.76 \pm 0.11$	$0.96 \pm 0.17$
	Left	$0.92 \pm 0.11$	$0.95 \pm 0.07$	$1.01 \pm 0.10$

**Table 2**

FSE signal in an axial plane of the thigh station. Reported values represent the mean  $\pm$  standard deviation of ratio of the anterior-right ROI divided by anterior-left ROI, for the diastolic and systolic phases of the cardiac cycle. The signal ratio was significantly different between the three groups and within each pair of groups ( $p < 0.0001$ ), except for the baseline and commercial pad pair which was not significantly different ( $p > 0.02$ ) for both cardiac phases.

Pad Setting		Baseline	Commercial Pad	High Permittivity Pad
FSE Signal Ratio	Diastolic	$0.48 \pm 0.14$	$0.59 \pm 0.14$	$0.80 \pm 0.21$
	Systolic	$0.49 \pm 0.13$	$0.60 \pm 0.15$	$0.88 \pm 0.19$

**Table 3**

Mean CNR and conspicuity scores for the right and left common femoral arteries. Reported values represent mean  $\pm$  standard deviation. In the right common femoral artery, the CNR and conspicuity scores were significantly different between the three groups and within each pair of groups ( $p < 0.0001$ ), whereas in the left common femoral artery the CNR and conspicuity scores were not significantly different between the groups ( $p > 0.5$ ).

	Pad Setting	Baseline	Commercial Pad	High Permittivity Pad
<b>Right</b>	<b>CNR</b>	12 $\pm$ 2	33 $\pm$ 8	82 $\pm$ 15
	<b>Conspicuity</b>	1.0 $\pm$ 0.0	2.5 $\pm$ 1.0	4.3 $\pm$ 0.8
<b>Left</b>	<b>CNR</b>	84 $\pm$ 13	78 $\pm$ 10	96 $\pm$ 17
	<b>Conspicuity</b>	4.5 $\pm$ 0.7	4.5 $\pm$ 0.7	4.5 $\pm$ 0.7